

# Collective Cargo Transport and Sorting with Molecular Swarms

Nathanael Aubert-Kato<sup>1</sup>, Geoff Nitschke<sup>2</sup>, Ibuki Kawamata<sup>3</sup> and Akira Kakugo<sup>4</sup>

<sup>1</sup>Department of Information Sciences  
Ochanomizu University, Tokyo, Japan  
naubertkato@is.ocha.ac.jp

<sup>2</sup>Computer Science Department  
University of Cape Town, South Africa  
gnitschke@cs.uct.ac.za

<sup>3</sup>Department of Robotics  
Tohoku University, Sendai, Japan  
ibuki.kawamata@tohoku.ac.jp

<sup>4</sup>Department of Physics  
Kyoto University, Japan  
kakugo.akira.8n@kyoto-u.ac.jp

## Abstract

Recent work has demonstrated the viability of DNA robotics and artificial molecular machines for molecular transportation and cargo sorting with potential applications in manufacturing responsive molecular devices, programmable therapeutics, and autonomous chemical synthesis. We extend previous work on cooperative molecular transportation using artificial molecular machines, where we similarly functionalize DNA-conjugated microtubules driven by kinesin motor proteins. DNA-functionalized microtubules propelled by surface-adhered kinesin motors enable the self-organization of molecular swarms, where such swarms load and transport cargo (microbead) in a simulated chemical environment. We demonstrate programmable molecular swarms for cargo sorting and cooperative transport. Cargo loading occurs when sufficient microtubules are at the same location as the cargo, and cargo unloading occurs at specific points in the environment through interaction with localized DNA species. Our contribution is the design of a chemotaxis molecular controller, forcing the swarm to tumble (random change direction) when the system is not following a molecular gradient corresponding to the cargo type, thus directing it to specific points for cargo unloading. This work thus contributes to the open problem of how to best design programmable molecular machines for various tasks in microscopic environments.

## Introduction

Molecular machines that perform mechanical tasks are key functional components in all biological organisms. The design and synthesis of artificial molecular machines (Balzani et al., 2000; Kay and Leigh, 2015; Hagiya et al., 2014) have promised various nanoscale and micro-scale applications including microscopic electric motors (Zhang and et al., 2023) and robotic swarms (Palagi and Fischer, 2018; Dorigo et al., 2020; VanSaders and Glotzer, 2021). Designing programmable molecular robots that automatically conduct complex (user-assigned) tasks in microscopic environments is a grand challenge in molecular engineering. Specifically, how to design molecular machines that are general problem solvers in microscopic environments (Thubagere and et al., 2017; Akter and et al., 2022).

Previous work has demonstrated the viability of fabricating many micro-robotic swarms using, for example, colloidal systems comprising active crystals or polymeric gels (Wang and et al., 2015; Xie and et al., 2019). Such swarming behavior can be directed using magnetic (Yan and et al., 2016) or electric fields (Palacci and et al., 2013), light (Katuri and et al., 2021; Akter and et al., 2022), or chemical signaling (Aubert-Kato et al., 2017; Zadorin et al., 2017) such that specific swarming behaviors emerge. Despite such advances in the design and synthesis of molecular machine swarms, microscale robots are still far from being capable of solving one of the grand visions of robotics – automated self-organization of swarm-robotic systems for solving various collective cooperative behavior tasks (Yang and et al., 2018), as currently envisioned by computational simulations (Yang and Bevan, 2020).

In this study, we demonstrate *in silico* one of such collective behavior tasks, cooperative cargo sorting, using simulated swarms of hundreds of biological molecular machines, specifically, microtubules propelled by kinesin motors as transporters. That task is a combination of behaviors that were previously demonstrated experimentally *in vitro*: collective cargo transport (Akter and et al., 2022) and molecular cargo sorting (Thubagere and et al., 2017). Here, multiple agents have to cooperate to transport different types of cargo to their designated target locations (Figure 1).

Akter and et al. (2022) use swarms of microtubules that can form bonds with each other and with the cargo (micro-beads) through the interaction of complementary DNA strands grafted to their surface. In their work, those DNA strands were chemically modified to integrate azobenzene molecules, which allowed them to break DNA-DNA bonds through interaction with UV light, and restored their binding abilities through interaction with visible light. By illuminating the target area with UV light, they were able to demonstrate experimentally the cooperative transport of cargo to a single target (Figure 1). The Akter and et al.

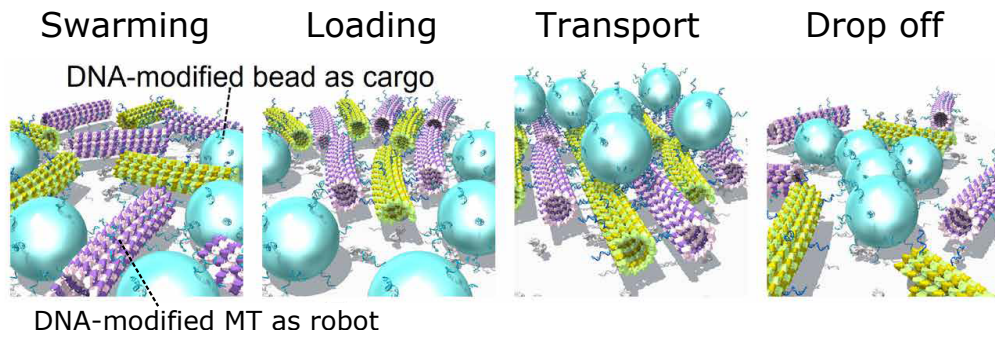


Figure 1: Illustration of the loading and transport of DNA-modified polystyrene beads as the model cargo (represented as cyan spheres) by the swarm of molecular transporters, adapted from (Akter and et al., 2022). Microtubules (MT) interact with each other through the hybridization of the DNA strands on their surface. Once a swarm large enough is formed, it may pick up cargo and transport it. Upon reaching the destination a physical mechanism (configuration switching of azobenzene in the original work; DNA strand displacement in this work) unloads the cargo.

(2022) approach has two limitations for the current task: (a) *their system cannot differentiate between different targets* and (b) *their system cannot sense the direction of the target area*. Using their approach, cargo is unloaded in any target area, regardless of its type, and is impossible to pick back up.

Thubagere and et al. (2017) demonstrated a simple molecular robot moving across a track made of DNA capable of picking up labeled cargo and dropping it off at its target location. As in the study of Akter and et al. (2022), cargo is picked through the interaction of complementary strands attached respectively to the robot and the cargo. In their case, the DNA strand attached to the cargo has a free section that can combine with the target, triggering the displacement of the cargo to the target (Figure 2). By design, their system does not allow for cooperation between agents, as they are incapable of walking together on the track.

### Contributions

This study extends the work of Akter and et al. (2022) by adding a target label, similar to the design of Thubagere and et al. (2017), to the DNA strand attached to the cargo, defining their type. Swarm formation occurs via physical interactions between microtubules (collisions) and the hybridization (that is, association) of DNA strands chemically attached to their surface. That hybridization is reversible but acts as a stabilizer for the swarm. Cargo loading happens at various points (initial cargo locations) and is based on the same interaction between DNA molecules. If the number of microtubules is large enough (dependent on the size and weight of the bead) the cargo will be loaded. The target areas have DNA strands attached to the surface, using the complementary sequence of the label of the expected cargo, similar to Thubagere and et al. (2017). Doing so solves issue (a) mentioned in the previous Section: the swarm can now differentiate between different types of cargo.

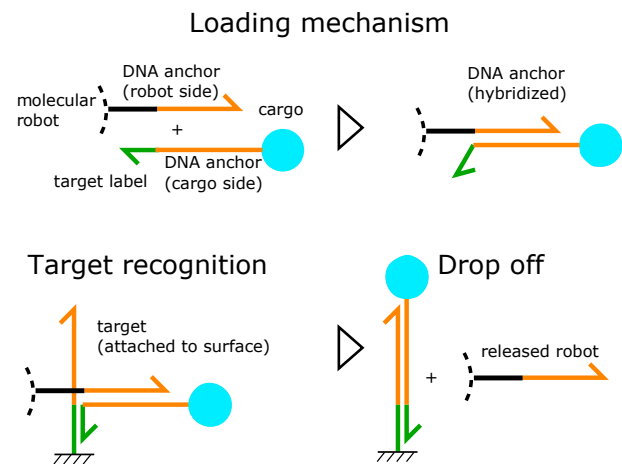


Figure 2: Loading and unloading of cargo based on transfers through DNA complementarity (strand displacement). DNA strands are represented as arrows corresponding to the 5' to 3' orientation. Colors show complementarity. Top: cargo is loaded on the molecular robot (microtubule) through the complementarity of anchoring sites. Bottom: single-stranded target site on the cargo hybridized to the DNA present in the target area, and cargo is unloaded via an exchange in the anchoring site (strand displacement). The anchoring site in the target strand is longer than that on the robot, making the exchange energetically favorable.

Finally, we add a molecular controller to the beads based on previous experimental work (Gines and et al., 2017; Aubert-Kato et al., 2017; Zadorin et al., 2017), implementing here the controller for a run-and-tumble-like strategy, thus providing some rudimentary chemotaxis. Tumbling is implemented by physically bending microtubules, thus forcing them to run in circles. At the same time, signal species are produced and diffused from the target area, providing a

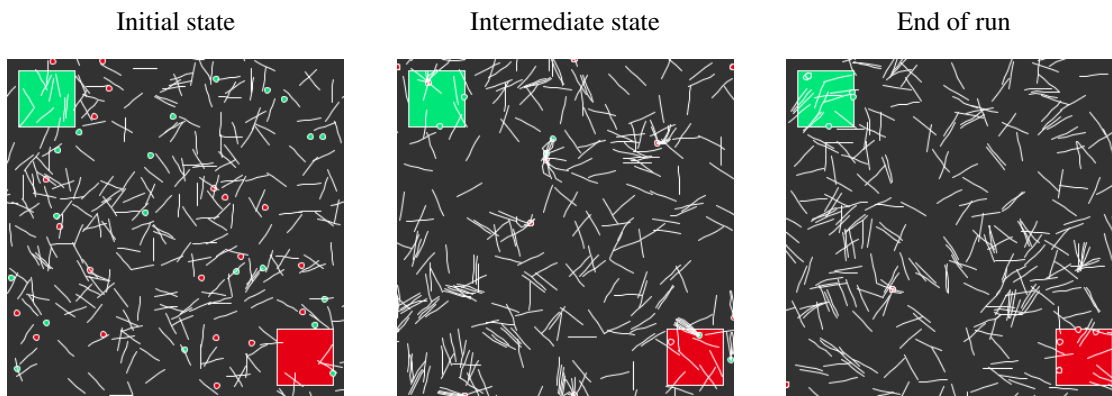


Figure 3: Environment. The microtubules are shown in white. The two targets are depicted as colored squares in opposite corners. Beads (cargo) are shown in the color that corresponds to their target. The initial state shows a typical distribution of cargo. The intermediate state shows swarms of microtubules, some of which have cargo loaded. At the end of a typical run, most beads have reached their target, while a few got stuck on the sides of the environment.

gradient to follow (Zadorin et al., 2017). Doing so solves issue (b): the swarm can sense the correct direction of the target, thus accelerating delivery compared to a random walk.

### Research Objective

Our objective is to demonstrate theoretically that the molecular swarm, with the extensions presented in the contribution, can solve the cooperative cargo sorting task. The swarm is to function in an environment with two cargo types, where the degree of cooperation (bead weight, thus affecting the number of robots required for transport) determines task complexity, and the amount of cargo (cooperatively) transported over time determines the collective behavior task performance (Figure 3).

This objective is evaluated with three cooperative difficulties and three types of controllers, for a total of nine configurations. For cooperative difficulty, we evaluate an environment containing a random uniform distribution of cargo with two cargo types (red and green) and two drop-off points (labeled with the same colors), where the bead weight is such that at least 1, 2 or 5 microtubules are required to transport cargo. The simplest case does not require cooperation, as a single microtubule can perform the task, but cooperation can still increase the movement speed of cargo, leading to improved performance. For controller types, we consider three cases:

- **No tumble**, which corresponds to no controller added to the beads. The system thus relies only on the random walk of the swarm to reach the target.
- **No gradient**, which corresponds to a controller that will periodically trigger the tumbling of the swarm carrying the bead, regardless of the change in distance to the target.

- **Gradient**, which corresponds to the same periodic molecular system, with an additional module sensing the change in the concentration of a signaling species. When the signal increases, the next oscillation is delayed, making the swarm remain on course. Note that the gradient sensing module only offers a delay; the controller will still trigger a tumble eventually even if the direction is correct.

This study demonstrates that tumbling is beneficial for task performance with respect to cooperative cargo sorting. However, we found that the impact of gradient sensing is dependent on the level of cooperation required. In some cases, periodic tumbling can be more beneficial than delayed tumbling, potentially due to the timing of the oscillations.

### Methods

This section describes the core methodology of our study, which comprises: the *agents* (swarming microtubules), the *cargo* (micro-beads) to be cooperatively transported, the *molecular framework* used to implement the controller (the PEN toolbox), and the simulation *environment*.

#### Molecular Environment and the PEN Toolbox

Our simulation environment<sup>1</sup> is designed to mirror that of previous work, with microtubules moving around, potentially forming swarms and interacting with cargo (Aker and et al., 2022). We set two specific areas in opposite corners as target unloading spots for the two different types of cargo (Figure 3). We also assume that they are the source of their respective molecular signal, diffusing in the environment (Aubert-Kato et al., 2017; Zadorin et al., 2017).

The core methodology of this study uses molecular programming (Adeleman, 1994), that is, using molecules

<sup>1</sup>Simulation source code and raw data are available at <https://doi.org/10.5281/zenodo.7947035>

(such as DNA, RNA, and proteins) to process information. Molecular programming relies on chemical concentrations to represent data and chemical reactions to transform data. There have been many *in vitro* demonstrations of molecular programming including computing a square root (Qian and Winfree, 2011), emulating neural networks (Qian et al., 2011), assembling DNA nanostructures (Seeman, 2003), encoding a toggle-switch (Padirac et al., 2012), cascaded DNA pattern formation (Abe et al., 2021), and a 2D predator-prey model (Padirac et al., 2013).

This study uses the PEN (*Polymerase, Exonuclease, Nickase*) toolbox (Montagne and et al., 2011), a molecular programming approach relying on the interaction between DNA molecules and enzymes to encode three basic operations (or modules): activation, inhibition, and degradation.

The PEN toolbox distinguishes between two types of DNA molecules: short (11 to 13 bases long) signal strands and longer (22 to 25 bases long) *template* strands. Signal strands can attach to complementary templates to produce other signal strands (activation), or temporarily inhibit activity (inhibition). Signal strands are continuously degraded by one of the enzymes (exonuclease), and template strands are chemically protected against degradation. As such, the concentration of signal strands changes through time depending on their interactions with the template strands.

PEN toolbox activation and inhibition modules can be combined in various ways to form programs that exhibit various behaviors, in both *in vitro* experiments, including an oscillator (Montagne and et al., 2011) and toggle switch (Padirac et al., 2012), and *in-silico* experiments (including a two-bit counter (Aubert and et al., 2020) and simple molecular robot controller (Hagiya et al., 2016)).

The efficacy of the PEN toolbox has been demonstrated using *in vitro* experiments including an approach that produced collective behaviors in thousands of agents, exhibiting fundamental mechanisms of living organisms including distributed decision-making and morphogenesis (Gines and et al., 2017). This work was the basis of later *in vitro* experiments (Aubert-Kato and et al., 2017; Zadorin et al., 2017) that demonstrated swarms of bio-micro-robots conceptualized as DNA-functionalized microbeads, with functionality to send and receive signals and self-assemble.

Thus, we chose to implement the molecular controller of our system with the PEN toolbox as it is chemically compatible with microtubules (Senoussi et al., 2021) and has been previously used *in vitro* in combination with microbeads, which we use as cargo in the present work.

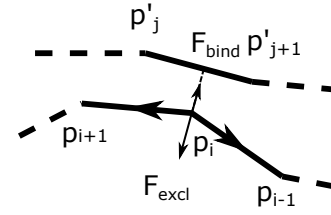


Figure 4: Interactions between microtubules, showing the forces exerted on segment extremity  $p_i$ . External forces ( $F_{bind}$  and  $F_{excl}$ ) are oriented as the normal to the segment applying them. Internal forces (interactions between ends of segments in the same microtubule) are shown as arrows along the segments. Dashed lines represent (potential) further segments. The forward force is not shown.

## Molecular Agents

Agents, in our simulation environment, correspond to individual microtubules gliding on the surface, propelled by molecular motors. While typical models of microtubules only focus on the position of their center of mass and orientation (see for instance Sumino et al. (2012) or Bär et al. (2020)), we need a more explicit model to capture interactions between microtubules and beads, as well as a way to represent their curvature when tumbling.

As such, we model microtubules as linearly jointed segments. We take inspiration from Kaneko et al. (2020) and assume each segment is a highly stiff spring connecting both of its extremities and simulate their movement by computing the forces applied to those extremities.

Formally, assuming a microtubule is a list  $(p_1, \dots, p_n)$  of  $n$  segment extremities, and assuming their "weight" is normalized to 1, the acceleration of  $i$ th extremity  $p_i$  is:

$$a_{p_i} = F_{internal} + \sum_{seg \sim p_i} (F_{excl}(seg, p_i) + F_{bind}(seg, p_i)) + \sum_{bead \sim p_i} F_{bind}(bead, p_i) \quad (1)$$

where  $seg \sim p_i$  and  $bead \sim p_i$  are the set of segments and beads in the neighborhood of  $p_i$ , respectively.  $F_{internal}$  corresponds to the spring forces from the one or two segments  $p_i$  belongs to. Each extremity is also subjected to two external forces: an exclusion force from nearby microtubules  $F_{excl}$  and a spring-like connecting force corresponding to the binding of DNA species on the surface of the microtubule to other microtubules or beads  $F_{bind}$ , similar to those in Akter and et al. (2022) (Figure 4).

Finally, the front extremity is subjected to a forward force, corresponding to the action of molecular motors

Experiment Parameters	
Required cooperation	1, 2 or 5
Controller types	No tumble No gradient Gradient
Runs (per experiment)	100
Task trial duration	200000 steps
Wrap around : Microtubules	Yes
Beads	No
Micro-tubules (swarm)	300
Bead initialization	Uniform random
Simulation Parameters	
1 spacial unit	250 nm
1 time step	0.5 s
Arena size	75 $\mu$ m x 75 $\mu$ m
Beads	5 per target
Bead radius (display)	1.25 $\mu$ m
Target size	12.5 $\mu$ m x 12.5 $\mu$ m
Interaction range	0.5 $\mu$ m
Microtubule length	5 $\mu$ m
Forward speed of microtubules	250 nm/s
Chemical Parameters	
Prey species production $V_{max}$	1000.0 $s^{-1}$
Prey species production $K_M$	200.0 (no unit)
Predation rate $p$	60.0 $s^{-1}$
Prey degradation rate $\lambda_N$	0.6 $s^{-1}$
Predator degradation rate $\lambda_P$	6.0 $s^{-1}$
Gradient degradation rate impact $\delta$	6.0 $s^{-1}$

Table 1: Experiment and Simulation Parameters

present on the surface of the environment. When tumbling, that force is instead angled by 90°.

We set the length of the microtubules in the simulation to be 5  $\mu$ m, moving with a base velocity of 250 nm·s<sup>-1</sup> based on values from the literature (Lüdecke et al., 2018). Beads are simulated to connect to nearby microtubules through a spring force corresponding to the binding of complementary DNA strands, similar to the interaction between microtubules. Bead weight has been normalized so that a weight of  $N$  requires  $N$  agents to effectively move across the environment.

### Cargo: Beads and molecular dynamics

Cargo in our system is implemented as microbeads distributed throughout the environment. As in previous work (Aker and et al., 2022), the beads are functionalized with DNA molecules, allowing collection by the swarm (agents) when in sufficiently close proximity.

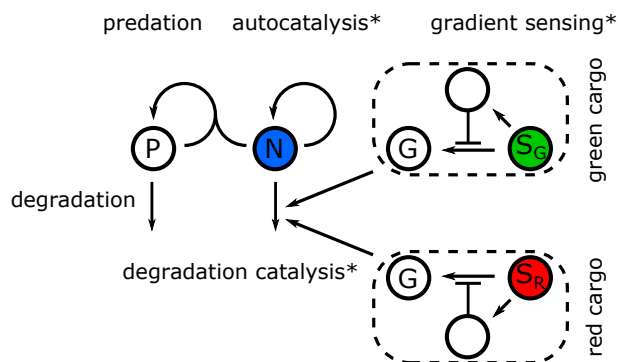


Figure 5: Reaction network of the molecular controller. Nodes are signal species, arrows represent templated reactions, and bar-headed arrows represent inhibitions in the PEN toolbox formalism. Elements marked by an asterisk (\*) are attached to the beads. The left part shows the simplified reaction network for the Predator-Prey oscillator (Fujii and Rondelez, 2013). The dashed sections implement an incoherent feed-forward network (Aubert et al., 2013), which responds to increases in the level of the beacon species  $S_G$  and  $S_R$  for the green and red cargo respectively. The output of that gradient sensing module is designed to increase the degradation rate of  $N$  (Montagne et al., 2016), changing oscillator behavior. Overall, beads will periodically produce spikes in the tumbling species  $N$ , except if they are moving towards increasing concentrations of their beacon species.

We also extend the method of Aker and et al. (2022) with additional DNA molecules implementing a molecular controller (Figure 5) based on the PEN toolbox. Figure 5 (left side), shows the simplified reaction network for the Predator-Prey oscillator (Fujii and Rondelez, 2013), where  $N$  corresponds to the tumbling species, consumed by species  $P$ , which in turn produces more of species  $P$  through the activity of the polymerase enzyme. Reaction network dynamics are as follows: templated autocatalysis increases the concentration of  $N$  over time. In turn, the predator species  $P$  multiplies over time by acting as a template to turn  $N$  molecules into more  $P$  molecules. As the concentration of  $P$  increases, the rate of predation eventually becomes higher than the production of  $N$ . Both species are progressively degraded over time by the exonuclease. Once the concentration of  $N$  gets too low, the degradation rate of  $P$  overcomes the predation rate, thus reducing its concentration to a level where the autocatalysis of  $N$  can pick up again, thus completing the cycle.

Additionally, the prey species  $N$  is designed to interact with DNA species present on the microtubules, inducing a strong asymmetry and forcing them to turn. While that extra interaction adds a load on the system, previous experimental work showed that oscillations can still occur (Dehne et al.,

2021). Note that the molecular program triggering the creation of all species involved in the oscillator is made of a single DNA molecule, which we attach to the bead.

The dashed sections (right side of Figure 5) are two copies of an incoherent feed-forward network (Aubert et al., 2013), which only produces an output in response to an increase in the level of a target-dependent beacon species ( $S_G$  or  $S_R$ ). When the signal is present, it combines with a PEN template species to create an output species. Concurrently, an inhibiting species is created, targeting that first template. Output is produced as long as the strength of the signal increases beyond the strength of the inhibition. Once the inhibition is too strong or if the signal's concentration decreases, no more output is produced, and both inhibitor and output are degraded over time, eventually resetting the system. This system requires two individual template species to be added to the bead. The output of that gradient sensing module is designed to increase the degradation rate of  $N$  (Montagne et al., 2016), thus delaying spikes in  $N$ .

As a result, the concentration of  $N$  will remain low for longer periods of time while moving toward the relevant target, thus allowing the swarm connected to the cargo to keep moving in a straight line. On the other hand, when the cargo is going in the wrong direction (no increase in the beacon species), the system will produce spikes at regular intervals, thus forcing the swarm to tumble and change direction. The concentration of the relevant species is computed through the following set of ordinary differential equations:

$$\begin{aligned} \frac{d[N]}{dt} &= \frac{V_{max} \cdot [N]}{K_M + [N]} - p \cdot [N][P] - (\lambda_N + \delta \cdot [G]) \cdot [N] \\ \frac{d[P]}{dt} &= p \cdot [N][P] - \lambda_P \cdot [P] \end{aligned} \quad (2)$$

Where  $[.]$  represents the concentration of a given species.  $G$  is the output of the gradient module (Figure 5). For the sake of simplicity, in the simulation,  $[G]$  is set to the improvement in distance to the target when moving towards it and 0 otherwise, while the molecular dynamics of the module itself is not computed.  $[G]$  is always set to 0 in the "no gradient" controller. Other parameters are explained in Table 1.

Finally, we extended the DNA strand used by the beads to attach to microtubules to have a toehold section allowing unloading once reaching the target area (Thubagere and et al., 2017). As such, the controller only requires one additional DNA species (no gradient) or three additional DNA species (gradient) compared to Akter and et al. (2022). We consider this design realistic since molecular programs of that size have been experimentally demonstrated *in vitro* to work even when grafted to microbeads (Gines and et al., 2017).

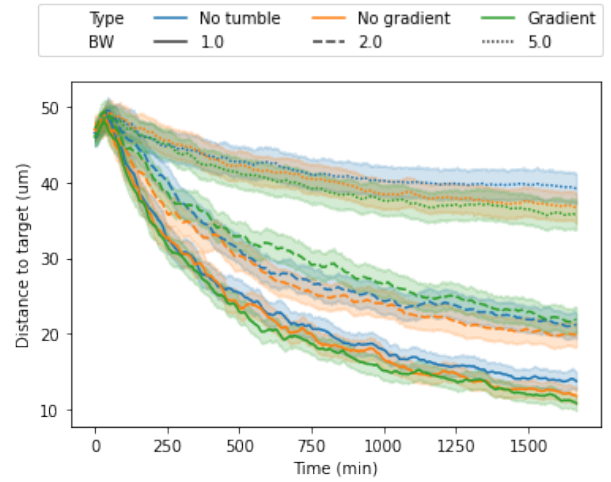


Figure 6: Distance over time of cargo for different controllers ("Type") and normalized bead weight ("BW"). Each configuration was run for 100 runs. Note that a distance from  $6.25\mu\text{m}$  (side) to  $8.8\mu\text{m}$  (corner) corresponds to a bead in the target area.

Agent, environment, cargo, and experiment parameters used in the simulation are summarized in Table 1.

## Experiments and Results

Experiments evaluated the efficacy of the molecular swarm for transporting labeled cargo to the relevant target area. We also investigated the relationship between the average task performance of the molecular controllers and the level of cooperation required to move the cargo. Experiments measured and recorded the distance between cargo and the center of their target area over time for all combinations of controller types (no tumble, tumbling without gradient sensing, and tumbling with gradient sensing) and cooperation constraints due to cargo weight (Figure 6). With the exception of the "no tumble" controller (that is, no control, change in direction only caused by interactions between microtubules) at the highest cooperation level, all simulated systems noticeably brought the cargo closer to their target.

For weight 1.0, the full system performs better than both no tumble and no gradient (which are comparable to each other). For weight 2.0, interestingly, the no gradient system performs the best, which corresponds to randomly forcing direction changes at regular intervals. For weight 5.0, both methods of tumbling are much better than no tumbling. As expected, the higher the weight, the more difficult it is for the swarm to coherently pick up the cargo and bring it to its destination. Note that, due to the chemical kinetics, the cargo is quickly dropped upon entry into the target area, meaning that the average distance would not converge towards 0 but rather towards a value close to the size of the

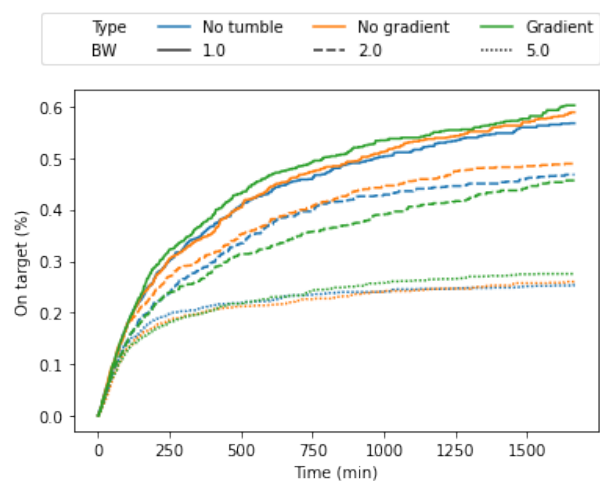


Figure 7: Average fraction of beads on target over time. Type corresponds to the controller type and BW to normalized Bead Weight.

target area. An additional limitation of using distance as a metric is that cargo may get stuck on the sides or corners of the arena, potentially in places that are close to the drop-off zone. As such, we also evaluated the actual fraction of cargo that reached their target over time (Figure 7).

The fraction was lower than what could be expected from the distance alone, confirming that some beads may get dropped near the target but not directly on it. Interestingly, the results show that the gradient-sensing method is lagging behind in the medium cooperation experiment. Visual inspection of the behavior of the swarms showed that they often tumbled just before reaching the target area. We investigated that behavior by looking at the concentration of the tumbling species over time, with and without the gradient sensing module (Figure 8).

The controller without gradient sensing (blue) provides regular oscillations similar to implementations of the system found in the literature (Fujii and Rondelez, 2013; Dehne et al., 2021). The addition of the gradient sensing module triggers a strong change in the behavior of the oscillations depending on the position of the bead with respect to its target and its current movement. In particular, we note that, even when moving in the correct direction, the oscillator will still eventually spike (which is expected), but at a much higher intensity than usual. That behavior may disaggregate the swarm, potentially dropping the cargo.

Additionally, once on target, side effects of the gradient sensing module will induce oscillations of higher amplitude than usual. Multiple cargoes dropped in close vicinity may be enough to force nearby swarms to tumble unex-

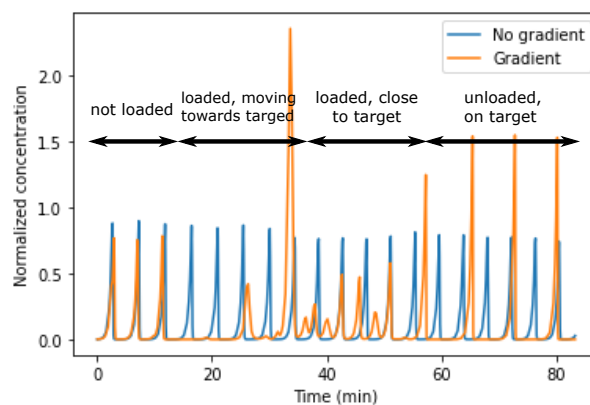


Figure 8: Concentration of the tumbling species  $N$  on a typical bead over time (orange). Concentration of the same species, without the gradient sensing module, is shown in blue for reference.

pectedly. Once again, that tumbling may disaggregate the swarm, dropping the cargo just outside the target area. That issue could be solved by adding a "kill switch" to the target area, preventing further oscillations from occurring.

## Conclusion

Scale in swarms has been shown to be a critical component in the emergence of complex behaviors (Witkowski and Ikegami, 2019). Molecular swarms with more than a million agents have been previously demonstrated (Aubert-Kato et al., 2017; Zadorin et al., 2017; Akter and et al., 2022), reaching the required scale. In this paper, we demonstrated that simple molecular programs can implement controllers for such swarms, leveraging emergent behavioral complexity. This study focused on a typical task from evolutionary robotics: the implementation of cooperative cargo sorting.

Our study combined simple molecular systems: a swarm of microtubules capable of the cooperative transport of cargo, and a gradient-sensing oscillator with the ability to physically bend microtubules, thus implementing a simple run-and-tumble strategy for chemotaxis. In particular, those elements were selected for their compatibility with the others in wet lab experiments.

We demonstrated that our system was indeed capable of solving the task at hand. The gradient sensing approach was generally beneficial compared to random movement. Unexpectedly, in the medium cooperation scenario, performing regular tumbles regardless of the gradient proved more beneficial than the gradient sensing approach, and both approaches had identical performance in the high cooperation scenario. We expect such results to be connected to the timing of oscillations compared to the movement of

the cargo and further behavioral improvements could be achieved through optimization of the controller's chemical parameters. Another potential reason comes from the fact that the gradient sensing mechanism lead to *stronger* spikes once the cargo was on target, which may force swarms to tumble just before reaching the goal. However, this could be addressed with a kill switch in the molecular controller.

In future work, we will attempt to scale up the number of agents in the simulation to provide results closer to the full capacities of molecular systems. The realism of the simulator can also be improved by explicitly computing the diffusion of molecular species through reaction-diffusion and by using more complex (but more realistic) models for the reaction kinetics (Aubert-Kato, 2020). Additionally, a systematic exploration of small reaction networks (2 to 5 template species) could yield a larger range of swarming behaviors (Cazenille et al., 2019).

### Acknowledgements

This work was supported by JSPS KAKENHI Grant Number JP21H04434.

Code and raw data availability: <https://doi.org/10.5281/zenodo.7947035>

### References

- Abe, K., Murata, S., and Kawamata, I. (2021). Cascaded pattern formation in hydrogel medium using the polymerisation approach. *Soft Matter*, 17(25):6160–6167.
- Aleman, L. (1994). Molecular computation of solutions to combinatorial problems. *Science*, 266(5187):1021–1024.
- Akter, M. and et al. (2022). Cooperative Cargo Transportation by a Swarm of Molecular Machines. *Science Robotics*, 65(7):DOI:10.1126/scirobotics.abm0677.
- Aubert, N., Dinh, Q., Hagiya, M., Fujii, T., Iba, H., Bredeche, N., and Rondelez, Y. (2013). Evolving cheating dna networks: a case study with the rock-paper-scissors game. In *European Conference on Artificial Life (ECAL-2013)*, pages 1–8.
- Aubert, N. and et al. (2020). Journal of The Royal Society Interface. *Computer-assisted design for scaling up systems based on DNA reaction networks*, 11(1):20131167.
- Aubert-Kato, N. and et al. (2017). Evolutionary optimization of self-assembly in a swarm of bio-micro-robots. In *Proceedings of the Genetic and Evolutionary Computation Conference*, pages 59–66, Berlin, Germany. ACM.
- Aubert-Kato, N., Fosseprez, C., Gines, G., Kawamata, I., Dinh, H., Cazenille, L., Estevez-Tores, A., Hagiya, M., Rondelez, Y.-N., and Bredeche, N. (2017). Evolutionary optimization of self-assembly in a swarm of bio-micro-robots. In *Proceedings of the Genetic and Evolutionary Computation Conference*, volume 8, pages 59–66, New York, NY, USA. ACM.
- Aubert-Kato, N. and Cazenille, L. (2020). New Generation Computing. *Designing Dynamical Molecular Systems with the PEN Toolbox*, 38(1):341–366.
- Balzani, V., et al., and et al. (2000). Artificial molecular machines. *Angewandte Chemie*, 39(1):3348–3391.
- Bär, M., Großmann, R., Heidenreich, S., and Peruani, F. (2020). Self-propelled rods: Insights and perspectives for active matter. *Annual Review of Condensed Matter Physics*, 11:441–466.
- Cazenille, L., Bredeche, N., and Aubert-Kato, N. (2019). Exploring self-assembling behaviors in a swarm of bio-micro-robots using surrogate-assisted map-elites. In *2019 IEEE Symposium Series on Computational Intelligence (SSCI)*, pages 238–246. IEEE.
- Dehne, H., Reitenbach, A., and Bausch, A. (2021). Reversible and spatiotemporal control of colloidal structure formation. *Nature Communications*, 12(1):6811.
- Dorigo, M., Theraulaz, G., and Trianni, V. (2020). Reflections on the future of swarm robotics. *Science Robotics*, 49(5):10080–10088.
- Fujii, T. and Rondelez, Y. (2013). Predator–prey molecular ecosystems. *ACS nano*, 7(1):27–34.
- Gines, G. and et al. (2017). Microscopic agents programmed by DNA circuits. *Nature Nanotechnology*, 12(1):351–359.
- Hagiya, M., Aubert-Kato, N., Wang, S., and Kobayashi, S. (2016). Molecular computers for molecular robots as hybrid systems. *Theoretical Computer Science*, 632:4–20.
- Hagiya, M., Konagaya, A., Kobayashi, S., Saito, H., and Murata, S. (2014). Molecular Robots with Sensors and Intelligence. *Accounts of Chemical Research*, 47(6):1681–1690.
- Kaneko, T., Furuta, K., Oiwa, K., Shintaku, H., Kotera, H., and Yokokawa, R. (2020). Different motilities of microtubules driven by kinesin-1 and kinesin-14 motors patterned on nanopillars. *Science Advances*, 6(4):eaax7413.
- Katuri, J. and et al. (2021). Inferring non-equilibrium interactions from tracer response near confined active Janus particles. *Science Advances*, 7(1):1–18.
- Kay, E. and Leigh, D. (2015). Rise of the molecular machines. *Angewandte Chemie*, 54(1):10080–10088.
- Lüdecke, A., Seidel, A.-M., Braun, M., Lansky, Z., and Diez, S. (2018). Diffusive tail anchorage determines velocity and force produced by kinesin-14 between crosslinked microtubules. *Nature communications*, 9(1):2214.
- Montagne, K. and et al. (2011). Programming an in vitro DNA oscillator using a molecular networking strategy. *Molecular systems biology*, 7(1):466.
- Montagne, K., Gines, G., Fujii, T., and Rondelez, Y. (2016). Boosting functionality of synthetic dna circuits with tailored deactivation. *Nature communications*, 7(1):13474.
- Padirac, A., Fujii, T., Estevez-Torres, A., and Rondelez, Y. (2013). Spatial waves in synthetic biochemical networks. *Journal of the American Chemical Society*, 39(135):14586–14592.
- Padirac, A., Fujii, T., and Rondelez, Y. (2012). Bottom-up construction of in vitro switchable memories. *Proceedings of the National Academy of Sciences*, 47(109):3212–3220.



- Palacci, J. and et al. (2013). Living crystals of lightactivated colloidal surfers. *Science*, 339(1):936–940.
- Palagi, S. and Fischer, P. (2018). Bioinspired microrobots. *Nature Reviews Materials*, 3(1):113–124.
- Qian, L. and Winfree, E. (2011). Scaling up digital circuit computation with DNA strand displacement cascades. *Science*, 332(6034):1196–1201.
- Qian, L., Winfree, E., and Bruck, J. (2011). Neural network computation with DNA strand displacement cascades. *Nature*, 475(7356):368–372.
- Seeman, N. (2003). DNA in a material world. *Nature*, 421(6921):427–431.
- Senoussi, A., Galas, J.-C., and Estevez-Torres, A. (2021). Programmed mechano-chemical coupling in reaction-diffusion active matter. *Science Advances*, 7(51):eabi9865.
- Sumino, Y., Nagai, K. H., Shitaka, Y., Tanaka, D., Yoshikawa, K., Chaté, H., and Oiwa, K. (2012). Large-scale vortex lattice emerging from collectively moving microtubules. *Nature*, 483(7390):448–452.
- Thubagere, A. and et al. (2017). A cargo-sorting DNA robot. *Science*, 357(eaan6558).
- VanSaders, B. and Glotzer, S. (2021). Sculpting crystals one burgers vector at a time: Toward colloidal lattice robot swarms. *PNAS*, 118(3):113–124.
- Wang, W. and et al. (2015). From one to many: Dynamic assembly and collective behavior of self-propelled colloidal motors. *Accounts of Chemical Research*, 48(1):1938–1946.
- Witkowski, O. and Ikegami, T. (2019). How to make swarms open-ended? evolving collective intelligence through a constricted exploration of adjacent possibles. *Artificial life*, 25(2):178–197.
- Xie, H. and et al. (2019). Reconfigurable magnetic microrobot swarm: Multimode transformation, locomotion, and manipulation. *Science Robotics*, 28(4):DOI:10.1126/scirobotics.abm0677.
- Yan, J. and et al. (2016). Reconfiguring active particles by electrostatic imbalance. *Nature Materials*, 15(1):1095–1099.
- Yang, G. and et al. (2018). The grand challenges of science robotics. *Science Robotics*, 14(3).
- Yang, Y. and Bevan, M. (2020). Cargo Capture and Transport by Colloidal Swarms. *Science Advances*, 6(4).
- Zadorin, A. S., Rondelez, Y., Gines, G., Dilhas, V., Urtel, G., Zambrano, A., Galas, J.-C., and Estevez-Torres, A. (2017). Synthesis and materialization of a reaction-diffusion french flag pattern. *Nature chemistry*, 9(10):990–996.
- Zhang, L. and et al. (2023). An electric molecular motor. *Nature*, 613(1):doi.org/10.1038/s41586-022-05421-6.